Variable Helix Elongation as a Tool to Modulate RNA Alignment and Motional Couplings

Elizabeth A. Dethoff[a], **Alexandar L. Hansen**[a,1], **Qi Zhang**[a,2], and **Hashim M. Al-Hashimi**[a,*]
[a]Department of Chemistry and Biophysics, University of Michigan, Ann Arbor, MI 48109, USA

[1]Departments of Molecular Genetics, Biochemistry, and Chemistry, University of Toronto, Toronto, Ontario, Canada, M5S 1A8

[2]Department of Chemistry and Biochemistry, University of California at Los Angeles, Los Angeles, CA 90095, USA

Abstract

The application of residual dipolar couplings (RDCs) in studies of RNA structure and dynamics can be complicated by the presence of couplings between collective helix motions and overall alignment and by the inability to modulate overall alignment of the molecule by changing the ordering medium. Here, we show for a 27-nt TAR RNA construct that variable levels of helix elongation can be used to alter both overall alignment and couplings to collective helix motions in a semi-predictable manner. In the absence of elongation, a four base-pair helix II capped by a UUCG apical loop exhibits a higher degree of order compared to a six base-pair helix I ($\vartheta_I/\vartheta_{II}$ = 0.56±0.1). The principal S_{zz} direction is nearly parallel to the axis of helix II but deviates by ~40° relative to the axis of helix I. Elongating helix I by three base-pairs equalizes the alignment of the two helices and pushes the RNA into the motional coupling limit such that the two helices have comparable degrees of order ($\vartheta_I/\vartheta_{II}$ = 0.92±0.04) and orientations relative to S_{zz} (~17°). Increasing the length of elongation further to twenty-two base-pairs pushes the RNA into the motional decoupling limit in which helix I dominates alignment ($\vartheta_{II}/\vartheta_I$ = 0.45±0.05), with S_{zz} orientated nearly parallel to its helix axis. Many of these trends can be rationalized using PALES simulations that employ a previously proposed three-state dynamic ensemble of TAR. Our results provide new insights into motional couplings, offer guidelines for assessing their extent, and suggest that variable degrees of helix elongation can allow access to independent sets of RDCs for characterizing RNA structural dynamics.

Keywords

Residual dipolar couplings; collective helix motions; transactivation response element; HIV

1. Introduction

There is great interest in utilizing NMR residual dipolar couplings (RDCs) [1,2] to characterize the structure and dynamics of biomolecules [3-5]. RDCs can be measured in molecules that are partially aligned, either spontaneously when they have a significant

---

magnetic susceptibility anisotropy [1,6] or, more commonly, by dissolution in an appropriate ordering medium [2,7-10]. Several studies have established the utility of measuring RDCs under multiple linearly independent alignment conditions [11] to increase the spatial resolution with which structure and dynamics can be simultaneously characterized [12-18].

Two challenges can arise when using RDCs to characterize the conformational dynamics of nucleic acids, particularly globally flexible RNAs. First, it cannot be generally assumed, as is done in most formalisms, that internal motions do not lead to coupled changes in overall alignment [12,13,19]. Rather, rigid-body collective movements of helical domains about flexible junctions can lead to significant changes in the RNA overall molecular shape and thus global alignment [20,21]. Second, though the alignment of proteins can be modulated by changing the alignment medium and altering the balance between electrostatic and steric forces governing alignment [11,22], this has proven difficult if not impossible for nucleic acids because their uniform charge distribution closely follows that of their molecular shape [23-28]. Although spontaneous magnetic field alignment can yield one additional independent alignment [26,28], the degree of order generally remains unfavorably small under current magnetic field strengths.

Recently, we showed that correlations between internal motions and overall alignment could be reduced and overall alignment altered by chemically perturbing the overall RNA molecular shape [20]. In particular, the alignment of the transactivation response element (TAR) RNA from HIV-1 dissolved in the Pf1 phage ordering medium [8,9] was modulated by independently elongating each of its two helices by twenty-two Watson-Crick base-pairs [20,29]. The elongation renders the overall molecular shape, and consequently overall alignment, far less sensitive to collective motions of helices. It also serves to predefine overall alignment by fixing the principal axis of order (S_{zz}) to be nearly parallel to the elongated helix axis. A similar mutagenesis strategy that serves to alter the surface electrostatic properties has successfully been used by Bax and co-workers to modulate the alignment of proteins [30].

In RNA, extensive helix elongation (>20 base-pairs) is generally required to adequately decouple internal and overall motions. However, this results in an unfavorable increase in the size of the RNA under study and also necessitates preparation of two specifically labeled samples to minimize spectral overcrowding from elongation residues [29]. Many RNAs, including TAR bound to ligands [31] or at high monovalent and divalent ion concentrations [32], are globally rigid and may not require extensive helix elongation to decouple motions. In these cases, moderate degrees of elongation may offer an approach for modulating alignment. Even for globally flexible RNAs, moderate elongation may help expose collective helix motions and provide physical insights into the motional couplings themselves [33]. Here, we examine the utility of moderate degrees of helix elongation in modulating both the alignment and degree of motional couplings in a TAR mutant, EI(3)-TAR_m, in which the apical wild-type loop has been replaced with a UUCG loop and in which the terminal helix is elongated by three base-pairs (Figure 1a).

2. Results and Discussion

We prepared uniformly ^{13}C/^{15}N labeled EI(3)-TAR_m by *in vitro* transcription as previously described [34]. As shown in Figure 1b, spectra of EI(3)-TAR_m are in excellent agreement with those of non-elongated TAR_m, indicating that the elongation does not affect its structural and dynamical integrity, as reported previously for a twenty-two base-pair elongated TAR sample (EI(22)-TAR_m, Figure 1a) [20,29]. A total of 9 N-H and 53 C-H RDCs (Table S1) were measured in sugar (C1′H1′) and base (C2H2, C5H5, C6H6, C8H8,

N1H1, and N3H3) moieties of EI(3)-TAR$_m$ using ~22 mg/ml of Pf1 phage as an ordering medium [8,35]. A plot of RDCs as a function of secondary structure is shown in Figure 2a and 2b for TAR$_m$ and EI(3)-TAR$_m$, respectively. The RDCs measured in helix I of TAR$_m$ are consistently attenuated relative to counterparts in helix II. This has previously been attributed to inter-helical motions and a smaller degree of order for helix I compared to helix II [36]. Differences between helix RDCs are far less pronounced in EI(3)-TAR$_m$, indicating that elongation of helix I by three base-pairs increases its degree of order relative to helix II. The poor agreement (R^2=0.61) observed between the EI(3)-TAR$_m$ and TAR$_m$ RDCs (Figure 2c) qualitatively suggests that the three-base pair elongation modulates overall alignment and/or motional couplings. An even poorer correlation (R^2=0.07) is observed upon elongating helix I by twenty-two base-pairs (Figure 2d), consistent with elongation-dependent modulation of alignment and/or motional couplings.

To characterize the alignment of EI(3)-TAR$_m$ in phage, we used the RDCs measured in non-terminal Watson-Crick base-pairs and structurally stable loop residues to determine order tensors for each helix. The order tensors were determined by fitting measured RDCs to an idealized A-form helical geometry and an X-ray structure of the loop[37] as described previously [38-40]. An excellent fit was observed between the measured and back-predicted RDCs, indicating that both EI(3)-TAR$_m$ helices are accurately modeled using an idealized A-form geometry as described previously for non-elongated [36] and elongated [20] TAR (Figure 2e).

In Figure 3a, we use a Sauson-Flamsteed map to depict the best-fit principal orientational solutions (S_{xx}, S_{yy}, and S_{zz}) obtained for each helix in EI(3)-TAR$_m$. The orientational solutions are shown relative to a molecular frame in which the helix axis is oriented along the molecular z direction. For comparison, the corresponding order tensors reported previously for TAR$_m$ [36] and EI(22)-TAR$_m$ [20] are also shown. The estimated uncertainty in the S_{zz} orientations determined for helix I/II using the program Aform-RDC [39] is 7°/6°, 2°/2°, and 2°/4° for TAR$_m$, EI(3)-TAR$_m$, and EI(22)-TAR$_m$, respectively. In TAR$_m$, S_{zz} deviates by only ~7° from the helix II axis but deviates by ~40° from the helix I axis. As expected, elongation of helix I by three base-pairs tips S_{zz} towards its helical axis such that S_{zz} deviates by only ~17° and is nearly fully aligned with the axis following a twenty-two base-pair elongation (~7°). The three S_{zz} directions in TAR$_m$, EI(3)-TAR$_m$, and EI(22)-TAR$_m$ do not fall along a common plane, most likely because the A-form helices deviate from perfect cylindrical axial symmetry (Figure 3a). The three base-pair elongation has an opposite, albeit smaller effect on helix II. The angle between S_{zz} and the helix II axis increases from ~7° to ~16° to ~32° upon elongation by three and twenty-two base-pairs, respectively (Figure 3a). Changes are also observed in the S_{xx} and S_{yy} orientations (Figure 3a) and the asymmetry parameter (η) (Figure S1a, S1b), indicating that elongation modulates all five elements of the order tensor.

Elongation of helix I leads to changes in relative degrees of helix order that mirror those observed for the principal S_{zz} direction. In TAR$_m$, helix II dominates overall alignment, yielding an internal generalized degree of order $\vartheta_{int} = \vartheta_I/\vartheta_{II} = 0.56\pm0.1$ that is consistent with large amplitude, inter-helical motions [36]. Elongating helix I by three base-pairs increases its level of order compared to helix II such that both helices now have comparable degrees of order ($\vartheta_{int} = \vartheta_I/\vartheta_{II} = 0.92\pm0.04$). This, together with the similar angles between the S_{zz} direction and the two helical axes (Figure 3a), strongly suggests that the three base-pair elongation equalizes contributions of the two helices to overall alignment and pushes TAR into the motional coupling limit. Extending the elongation of helix I to twenty-two base-pairs drives the system towards the decoupling limit in which helix I dominates alignment ($\vartheta_{int} = \vartheta_{II}/\vartheta_I = 0.45\pm0.05$). Because RNA helices are often not coaxially stacked, moderate degrees of elongation are expected to modulate alignment. This was verified using

PALES simulations on a variety of RNAs following elongation of the terminal helix by three base-pairs (data not shown). The combination of helix-elongation with measurements of magnetic field-induced RDCs [26,28] may make it possible to access the maximum of five linearly independent sets of RDCs in nucleic acids. Access to such measurements will make it possible to more fully characterize the structural dynamics of RNA.

To rationalize the observed trends in the alignment of TAR as a function of elongation, we used the three-state dynamical ensemble determined previously using RDCs [20] in conjunction with electrostatic-induced alignment simulations using the program PALES [23,41] to simulate TAR alignment in phage at varying lengths of helix I elongation. The three-state ensemble is a discrete approximation of what is likely a continuous distribution involving many conformations. While we do not expect to observe quantitative agreement between measured alignment parameters and values predicted using this three-state ensemble approximation, we would like to obtain insights into the general trends observed for orientation and alignment upon helix elongation. An elongated helix I was superimposed onto each of the three TAR conformers of the ensemble, and PALES was used to predict the RDCs for each conformer. Bulge residues were not included in the three-state dynamical ensemble, so they were not included in PALES calculations. The three sets of RDCs simulated for each conformer were then averaged and used to compute order tensors for each helix. As shown in Figure 3a, we observe very good agreement between measured and predicted S_{zz} directions. The deviations range between 2-11° and 6-8°, for helices I and II, respectively. The simulations reproduce the observed non-planar approach of the S_{zz} direction towards the helix I axis with increasing elongation. Interestingly, the S_{xx} and S_{yy} directions (Figure 3a) and the asymmetry (Figure S1) are also reasonably well reproduced considering their much larger experimental uncertainty and given that exclusion of the bulge has a strong effect on these predicted values (data not shown). The simulations reproduce the increase in the helix I order compared to helix II upon helix I elongation (Figure 3b). Also, the simulated ϑ_{int} values reflect the observed trend. The larger discrepancy in TAR_m could arise from neglect of the bulge and fraying motions at terminal base-pairs which are likely to have a bigger effect on the small TAR_m compared to the other elongated constructs. Indeed, better agreement is observed for TAR_m when excluding the two terminal base-pairs in helix I (Figure 3b).

Independent RDC data sets are often used to overcome the 4^{n-1} fold orientational degeneracy arising from superposition of the order tensors of *n* domains [11,22]. One of the consequences of having differential motional averaging effects due to inter-domain motions is that two sets of RDCs may not be reconcilable with a single inter-domain orientation [42]. This is the case for the RDC datasets measured in TAR_m, EI(3)-TAR_m, and EI(22)-TAR_m. As shown in Figure 4a, none of the four inter-helix structures assembled using the RDCs measured in TAR_m satisfy the orientational solutions obtained using the EI(3)-TAR_m RDCs. Similarly, a common solution does not exist when using RDCs from EI(22)-TAR_m (Figure 4b). Thus, the inability to reconcile RDCs measured in differentially elongated RNAs in this manner may be an indication that inter-helix motions are present. However, other sources of experimental uncertainty should also be ruled out.

3. Conclusion

In conclusion, we show that modest degrees of helix-elongation can be used to modulate both overall alignment of RNA and the degree of motional couplings in a semi-predictable manner. Our results underscore the importance of exercising caution in interpreting similar levels of order for two domains (ϑ_{int} ~1) in terms of inter-domain rigidity. In general, motional couplings obscure inter-domain motion and will often result in underestimated dynamics. Our data suggest that even moderate degrees of helix elongation may be used to

push an RNA system outside the motionally coupled regime, though the degree of elongation needed will obviously vary from RNA to RNA.

Supplementary Material

Refer to Web version on PubMed Central for supplementary material.

Acknowledgments

References

1. Tolman JR, Flanagan JM, Kennedy MA, Prestegard JH. Nuclear magnetic dipole interactions in field-oriented proteins - information for structure determination in solution. Proc Natl Acad Sci USA. 1995; 92:9279–9283. [PubMed: 7568117]

2. Tjandra N, Bax A. Direct measurement of distances and angles in biomolecules by NMR in a dilute liquid crystalline medium. Science. 1997; 278:1111–1114. [PubMed: 9353189]

3. Tolman JR, Ruan K. NMR residual dipolar couplings as probes of biomolecular dynamics. Chem Rev. 2006; 106:1720–36. [PubMed: 16683751]

4. Bouvignies G, Markwick PR, Blackledge M. Simultaneous definition of high resolution protein structure and backbone conformational dynamics using NMR residual dipolar couplings. Chemphyschem. 2007; 8:1901–9. [PubMed: 17654630]

5. Getz M, Sun X, Casiano-Negroni A, Zhang Q, Al-Hashimi HM. NMR studies of RNA dynamics and structural plasticity using NMR residual dipolar couplings. Biopolymers. 2007; 86:384–402. [PubMed: 17594140]

6. Bothner-By, AA. Magnetic field induced alignment of molecules. In: Grant, DM.; Harris, RK., editors. Encyclopedia of Nuclear Magnetic Resonance. Wiley; Chichester: 1995. p. 2932-2938.

7. Bax A, Grishaev A. Weak alignment NMR: a hawk-eyed view of biomolecular structure. Curr Opin Struct Biol. 2005; 15:563–70. [PubMed: 16140525]

8. Clore GM, Starich MR, Gronenborn AM. Measurement of residual dipolar couplings of macromolecules aligned in the nematic phase of a colloidal suspension of rod-shaped viruses. J Am Chem Soc. 1998; 120:10571–10572.

9. Hansen MR, Hanson P, Pardi A. Filamentous bacteriophage for aligning RNA, DNA, and proteins for measurement of nuclear magnetic resonance dipolar coupling interactions. Meth Enzymol. 2000; 317:220–240. [PubMed: 10829283]

10. Ruckert M, Otting G. Alignment of biological macromolecules in novel nonionic liquid crystalline media for NMR experiments. J Am Chem Soc. 2000; 122:7793–7797.

11. Ramirez BE, Bax A. Modulation of the alignment tensor of macromolecules dissolved in a dilute liquid crystalline medium. J Am Chem Soc. 1998; 120:9106–9107.

12. Ruan K, Briggman KB, Tolman JR. De novo determination of internuclear vector orientations from residual dipolar couplings measured in three independent alignment media. J Biomol NMR. 2008; 41:61–76. [PubMed: 18478335]

13. Peti W, Meiler J, Bruschweiler R, Griesinger C. Model-free analysis of protein backbone motion from residual dipolar couplings. J Am Chem Soc. 2002; 124:5822–33. [PubMed: 12010057]

14. Bouvignies G, Markwick P, Bruschweiler R, Blackledge M. Simultaneous determination of protein backbone structure and dynamics from residual dipolar couplings. J Am Chem Soc. 2006; 128:15100–1. [PubMed: 17117856]

15. Clore GM, Schwieters CD. Amplitudes of protein backbone dynamics and correlated motions in a small alpha/beta protein: correspondence of dipolar coupling and heteronuclear relaxation measurements. Biochemistry. 2004; 43:10678–91. [PubMed: 15311929]

16. Lange OF, Lakomek NA, Fares C, Schroder GF, Walter KF, Becker S, Meiler J, Grubmuller H, Griesinger C, de Groot BL. Recognition dynamics up to microseconds revealed from an RDC-derived ubiquitin ensemble in solution. Science. 2008; 320:1471–5. [PubMed: 18556554]

17. Tolman JR. A novel approach to the retrieval of structural and dynamic information from residual dipolar couplings using several oriented media in biomolecular NMR spectroscopy. J Am Chem Soc. 2002; 124:12020–30. [PubMed: 12358549]

18. Meiler J, Prompers JJ, Peti W, Griesinger C, Bruschweiler R. Model-free approach to the dynamic interpretation of residual dipolar couplings in globular proteins. J Am Chem Soc. 2001; 123:6098–6107. [PubMed: 11414844]

19. Briggman KB, Tolman JR. De novo determination of bond orientations and order parameters from residual dipolar couplings with high accuracy. J Am Chem Soc. 2003; 125:10164–5. [PubMed: 12926926]

20. Zhang Q, Stelzer AC, Fisher CK, Al-Hashimi HM. Visualizing spatially correlated dynamics that directs RNA conformational transitions. Nature. 2007; 450:1263–7. [PubMed: 18097416]

21. Zhang Q, Throolin R, Pitt SW, Serganov A, Al-Hashimi HM. Probing motions between equivalent RNA domains using magnetic field induced residual dipolar couplings: accounting for correlations between motions and alignment. J Am Chem Soc. 2003; 125:10530–1. [PubMed: 12940730]

22. Al-Hashimi HM, Valafar H, Terrell M, Zartler ER, Eidsness MK, Prestegard JH. Variation of molecular alignment as a means of resolving orientational ambiguities in protein structures from dipolar couplings. J Magn Reson. 2000; 143:402–406. [PubMed: 10729267]

23. Zweckstetter M, Bax A. Prediction of sterically induced alignment in a dilute liquid crystalline phase; aid to protein structure determination by NMR. J Am Chem Soc. 2000; 122:3791–3792.

24. Zweckstetter M, Hummer G, Bax A. Prediction of charge-induced molecular alignment of biomolecules dissolved in dilute liquid-crystalline phases. Biophys J. 2004; 86:3444–60. [PubMed: 15189846]

25. Wu B, Petersen M, Girard F, Tessari M, Wijmenga SS. Prediction of molecular alignment of nucleic acids in aligned media. J Biomol NMR. 2006; 35:103–115. [PubMed: 16718586]

26. Al-Hashimi HM, Majumdar A, Gorin A, Kettani A, Skripkin E, Patel DJ. Field- and phage-induced dipolar couplings in a homodimeric DNA quadruplex, relative orientation of G·(C-A) triad and G-tetrad motifs and direct determination of C2 symmetry axis orientation. J Am Chem Soc. 2001; 123:633–640. [PubMed: 11456575]

27. Vermeulen A, McCallum SA, Pardi A. Comparison of the global structure and dynamics of native and unmodified tRNA^{val}. Biochemistry. 2005; 44:6024–33. [PubMed: 15835891]

28. Latham MP, Hanson P, Brown DJ, Pardi A. Comparison of alignment tensors generated for native tRNA(Val) using magnetic fields and liquid crystalline media. J Biomol NMR. 2008; 40:83–94. [PubMed: 18026844]

29. Zhang Q, Sun X, Watt ED, Al-Hashimi HM. Resolving the motional modes that code for RNA adaptation. Science. 2006; 311:653–6. [PubMed: 16456078]

30. Yao L, Bax A. Modulating protein alignment in a liquid-crystalline medium through conservative mutagenesis. J Am Chem Soc. 2007; 129:11326–7. [PubMed: 17718572]

31. Pitt SW, Zhang Q, Patel DJ, Al-Hashimi HM. Evidence that electrostatic interactions dictate the ligand-induced arrest of RNA global flexibility. Angew Chem Int Ed Engl. 2005; 44:3412–5. [PubMed: 15861447]

32. Casiano-Negroni A, Sun X, Al-Hashimi HM. Probing Na^{+}-induced changes in the HIV-1 TAR conformational dynamics using NMR residual dipolar couplings: new insights into the role of counterions and electrostatic interactions in adaptive recognition. Biochemistry. 2007; 46:6525–35. [PubMed: 17488097]

33. Zhang Q, Al-Hashimi HM. Extending the NMR spatial resolution limit for RNA by motional couplings. Nat Methods. 2008; 5:243–5. [PubMed: 18246076]

34. Dethoff EA, Hansen AL, Musselman C, Watt ED, Andricioaei I, Al-Hashimi HM. Characterizing complex dynamics in the transactivation response element apical loop and motional correlations with the bulge by NMR, molecular dynamics, and mutagenesis. Biophys J. 2008; 95:3906–15. [PubMed: 18621815]

35. Hansen MR, Mueller L, Pardi A. Tunable alignment of macromolecules by filamentous phage yields dipolar coupling interactions. Nat Struc Biol. 1998; 5:1065–1074.

36. Al-Hashimi HM, Gosser Y, Gorin A, Hu W, Majumdar A, Patel DJ. Concerted motions in HIV-1 TAR RNA may allow access to bound state conformations: RNA dynamics from NMR residual dipolar couplings. J Mol Biol. 2002; 315:95–102. [PubMed: 11779230]

37. Ennifar E, Nikulin A, Tishchenko S, Serganov A, Nevskaya N, Garber M, Ehresmann B, Ehresmann C, Nikonov S, Dumas P. The crystal structure of UUCG tetraloop. J Mol Biol. 2000; 304:35–42. [PubMed: 11071808]

38. Al-Hashimi HM, Gorin A, Majumdar A, Gosser Y, Patel DJ. Towards structural Genomics of RNA: Rapid NMR resonance assignment and simultaneous RNA tertiary structure determination using residual dipolar couplings. J Mol Biol. 2002; 318:637–649. [PubMed: 12054812]

39. Musselman C, Pitt SW, Gulati K, Foster LL, Andricioaei I, Al-Hashimi HM. Impact of static and dynamic A-form heterogeneity on the determination of RNA global structural dynamics using NMR residual dipolar couplings. J Biomol NMR. 2006; 36:235–49. [PubMed: 17077936]

40. Bailor MH, Musselman C, Hansen AL, Gulati K, Patel DJ, Al-Hashimi HM. Characterizing the relative orientation and dynamics of RNA A-form helices using NMR residual dipolar couplings. Nat Protoc. 2007; 2:1536–46. [PubMed: 17571061]

41. Zweckstetter M. NMR: prediction of molecular alignment from structure using the PALES software. Nat Protoc. 2008; 3:679–90. [PubMed: 18388951]

42. Tolman JR, Al-Hashimi HM, Kay LE, Prestegard JH. Structural and dynamic analysis of residual dipolar coupling data for proteins. J Am Chem Soc. 2001; 123:1416–1424. [PubMed: 11456715]

43. Sun X, Zhang Q, Al-Hashimi HM. Resolving fast and slow motions in the internal loop containing stem-loop 1 of HIV-1 that are modulated by Mg^{2+} binding: role in the kissing-duplex structural transition. Nucleic Acids Res. 2007; 35:1698–713. [PubMed: 17311812]
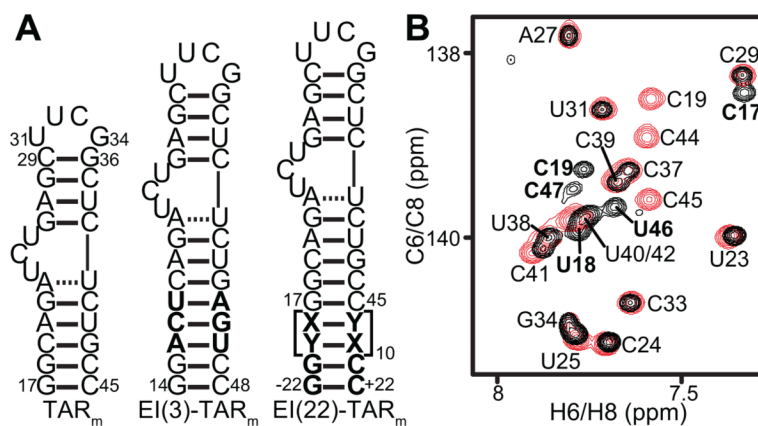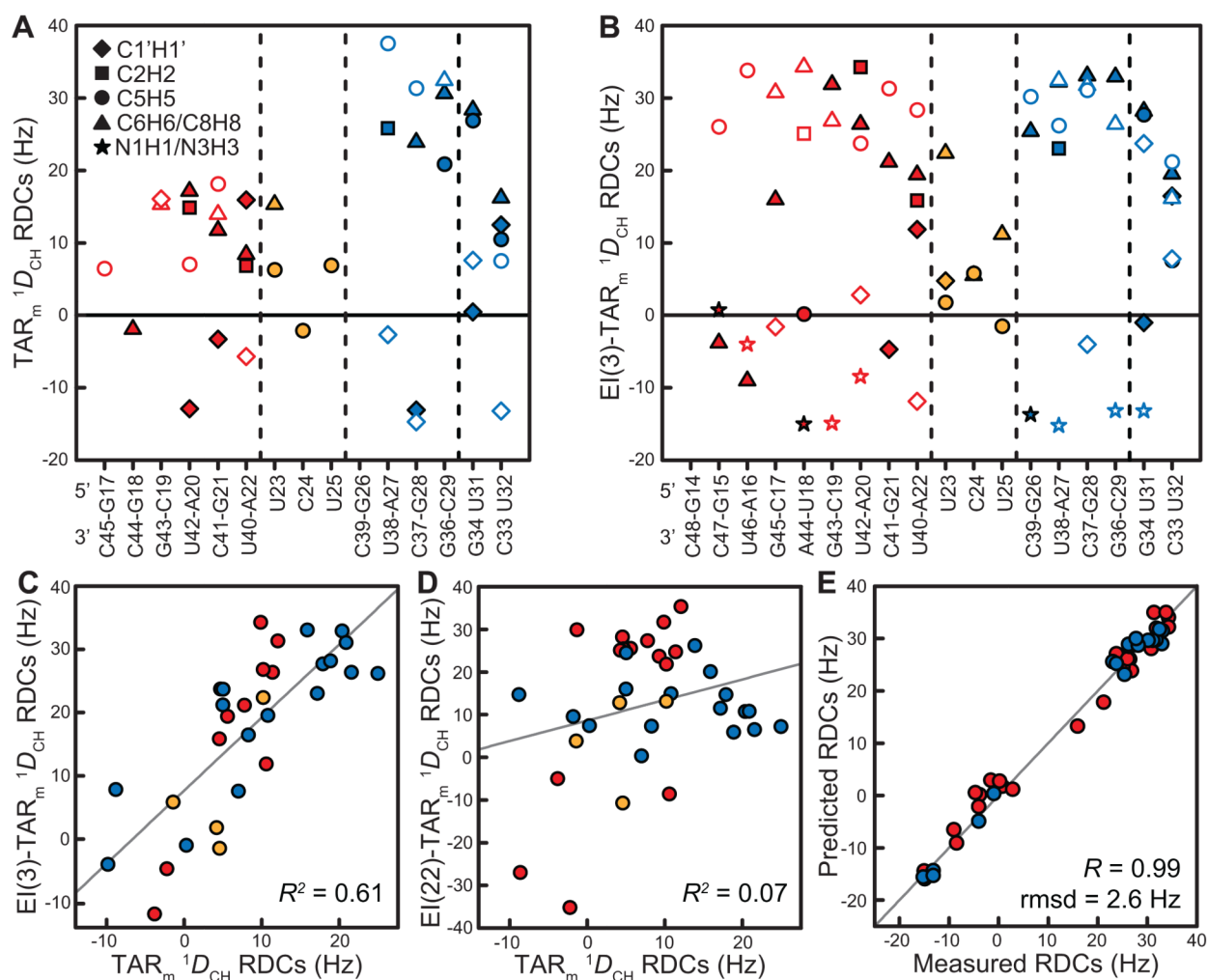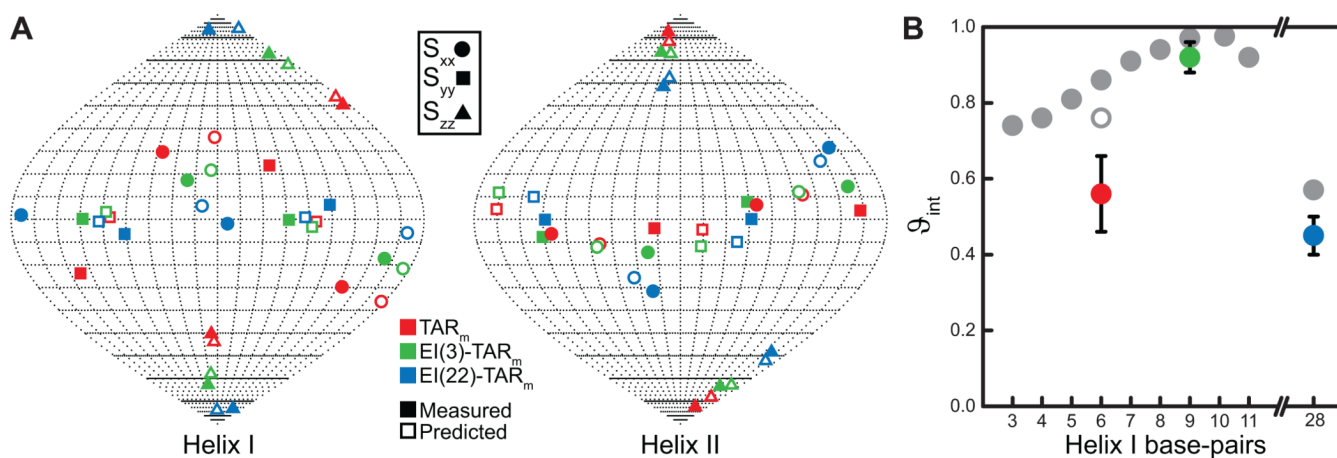
Figure 1.
TAR$_m$ constructs. (a) Secondary structures of TAR$_m$, EI(3)-TAR$_m$, and EI(22)-TAR$_m$. Differences between constructs are shown in bold. (b) 2D ^{1}H-^{13}C HSQC spectrum of EI(3)-TAR$_m$ (black) overlaid on the corresponding spectrum of TAR$_m$ (red). TAR$_m$ resonances are labeled in black, while peaks that belong only to EI(3)-TAR$_m$ are shown in bold. All EI(3)-TAR$_m$ experiments were conducted in NMR buffer (15 mM sodium phosphate, 25 mM sodium chloride, 0.1 mM EDTA and pH 6.4) at 298 K on an Avance Bruker 600 MHz NMR spectrometer equipped with a triple-resonance 5 mm cryogenic probe. ^{1}H, ^{13}C, and ^{15}N resonances were assigned by spectra overlay [29,43] and using standard homonuclear and heteronuclear 2D experiments, including an exchangeable NOESY and a 2D HCN experiment that correlates intranucleotide H8/H6 to N1/N9 to H1′.

Figure 2.
Measurement of RDCs in EI(3)-TAR$_m$. One bond RDCs ($^1D_{CH}$ and $^1D_{NH}$) measured in (a) TAR$_m$ and (b) EI(3)-TAR$_m$ as a function of residue/secondary structure. Filled and open circles represent RDCs measured on the 5′and 3′ strand, respectively. RDCs have been normalized to those of EI(3)-TAR$_m$ by the ratio of the ϑ_{II} values of EI(3)-TAR$_m$ and TAR$_m$. See inset in Figure 2a for key. (c-d) Correlation plots between (c) TAR$_m$ and EI(3)-TAR$_m$ and (d) TAR$_m$ and EI(22)-TAR$_m$ RDCs. (e) Comparison of EI(3)-TAR$_m$ RDCs measured in helix I (red) and helix II (blue) with values back-predicted using the best-fit order tensor and an idealized A-form helix and X-ray structure of the loop.

Figure 3.
Measured and predicted alignment of variable elongated TAR. (a) Sauson-Flamsteed maps showing the best-fit measured (filled symbols) and PALES-predicted (open symbols) order tensor frames (S_{xx}, S_{yy}, and S_{zz}) for helices I and II. Solutions are depicted relative to a molecular frame in which the helix axis is oriented along the z direction. (b) Measured (in color) and PALES-predicted (in gray) ϑ_{int} values ($\vartheta_{int} = \vartheta_{II}/\vartheta_{I}$) as a function of helix I length. Note that the value for EI(22)-TAR_m corresponds to $\vartheta_{int} = \vartheta_{I}/\vartheta_{II}$. The open circle corresponds to the predicted ϑ_{int} value of TAR_m when the two terminal base-pairs are excluded.
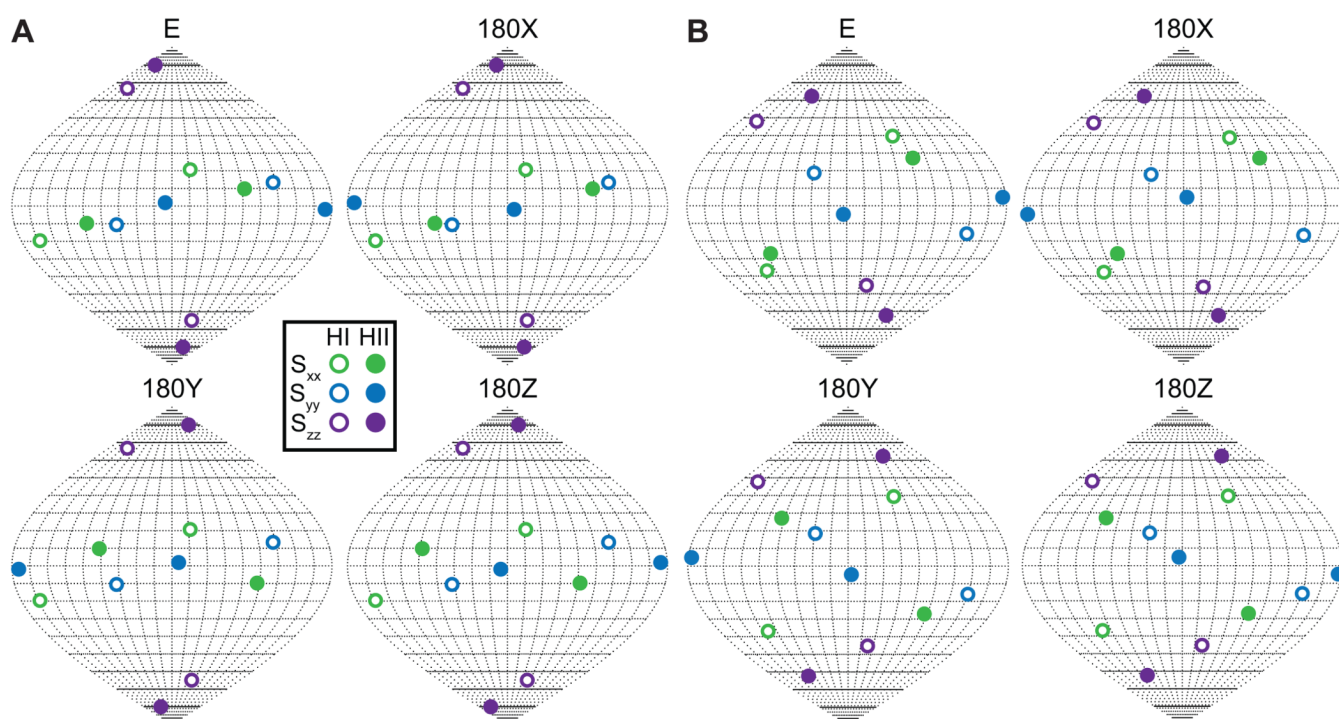
Figure 4.
Difficulty in resolving degeneracies in determining the average orientation of TAR helices using multiple RDC data sets. Shown are the experimental order tensor frames (S_{xx}, S_{yy}, and S_{zz}, in green, blue, and purple, respectively) determined for helix I (open circles) and II (filled circles) using (a) EI(3)-TAR_m and (b) EI(22)-TAR_m RDCs shown relative to the PAS of the order tensor determined using the TAR_m RDCs. The different orientational solutions were generated by rotating helix II in the TAR_m PAS 180° degrees about the x, y, and z axis.